Inter and Intrastrand Vibrational Coupling in DNA Studied with Heterodyned 2D-IR Spectroscopy

Amber T. Krummel, Prabuddha Mukherjee, and Martin T. Zanni*

Department of Chemistry, University of Wisconsin—Madison, Madison, Wisconsin 53706-1396

Received: May 27, 2003; In Final Form: July 7, 2003

Heterodyned 2D-IR, frequency resolved photon echo, and pump−probe spectroscopies were collected to study the couplings and anharmonicities of cytidine and guanosine bases in DNA. Cytidine and guanosine anharmonicities were measured to be 9 and 14 cm^{-1}, respectively. Strong cross-peaks were observed between the guanosine (G) and cytosine (C) carbonyl stretches in the 2D-IR spectra of the self-complementary oligonucleotide dG_5C_5 (5′-GGGGGCCCCC-3′). The spectra are interpreted in terms of inter- and intrastrand couplings between the carbonyl modes, and an excitonic Hamiltonian, based on transition dipole coupling, was used to fit the 2D-IR spectra. The accuracy of this model is discussed in light of observed couplings to the ring modes.

New multidimensional laser spectroscopies are beginning to be developed that are capable of measuring the anharmonic terms in the potential energy surface not readily accessible to linear spectroscopies.[1−11] These terms are the result of mechanical and electrostatic couplings between the normal modes of the molecule, and are thus sensitive to the molecular structure. In the case where the anharmonicities are dominated by mechanical coupling mechanisms, deducing the molecular structure from the frequencies and anharmonicities is difficult, because the potential is a complicated function of nuclear coordinates.[12] However, in the case where electrostatic coupling dominates, it is more likely that the higher order terms can be described by a simple model, such as a transition dipole or transition charge model.[13] In this Letter, we report the first application of 2D-IR spectroscopy to DNA and present a preliminary interpretation of the spectra with regard to mechanical and electrostatic coupling mechanisms.

The infrared spectra of DNA oligomers in the region of the base carbonyl stretches are known to be sensitive to the 3D structure of DNA.[14] Each of the four bases of DNA has a unique vibrational frequency that shifts upon duplex formation.[15] For example, in poly(dG)·poly(dC), the guanosine (G) and cytidine (C) carbonyl frequencies shift +21 and −2 cm^{-1}, respectively, suggesting strong vibrational coupling,[16] although the origin of the coupling is unknown. Transition dipole coupling has been proposed to explain shifts in poly(adenosine)·poly(uridine) helices,[17] but in neither case has a model been developed that accounts for both the intrastrand coupling among stacked bases and the interstrand coupling between hydrogen-bonded bases. We use heterodyned 2D-IR spectroscopy to measure the coupling between the carbonyl stretch bands of G and C bases (structure I) in double-stranded dG_5C_5. Using additional information from frequency resolved photon echo and pump−probe spectroscopies, we simulate the spectra using an exciton model and transition dipole coupling.

A detailed description of the methods will be given elsewhere.[18] Briefly, a difference frequency optical parametric amplifier generates ∼6 μm, 120 fs, 2 μJ pulses that are split into four beams, three of which (k_1, k_2, and k_3) generate a photon echo and the fourth overlaps the echo in the $k_{LO} = -k_1 + k_2 +$ k_3 phase matching direction. The four pulses are separated by time t_1, t_2, and t_3 and have polarizations $\langle p_1,p_2,p_3,p_{LO}\rangle$. The time delays t_1 and t_3 were scanned with $t_2 = 0$ and the signal Fourier transformed to generate the 2D-IR spectra.[19] The frequency axes of the spectra were calibrated using the linear spectrum along ω_1 and the frequency resolved photon echo along ω_3. Pump−probe and frequency resolved echo signals were obtained by dispersing the third-order signal in a monochromator. The samples dCMP (2′-deoxycytidine-5′-monophosphate, 50 mM), dGMP (2′-deoxyguanosine-5′-monophosphate, 50 mM), and self-complementary dG_5C_5 (5′-GGGGGCCCCC-3′, 500 μM) were buffered in 50 mM NaCl/50 mM potassium phosphate in D_2O with pD = 6.9.[20] dG_5C_5 was annealed to induce helix formation and is in the A-form.[21]

Structure I

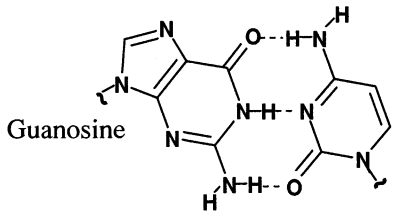

Linear and absolute value 2D-IR spectra of dG_5C_5 are shown in Figure 1a−d.[22] Four diagonal peaks are observed in the 2D-IR spectra, labeled A−D, corresponding to the G and C ring modes at 1584 and 1621 cm^{-1}, respectively, and the carbonyl stretches of C and G at 1650 and 1682 cm^{-1}, respectively. In dG_5C_5, G is 18 cm^{-1} higher than in dGMP, and C has the same frequency as dCMP. Peaks E and F are cross-peaks between the carbonyl modes, and peaks G−J are cross-peaks between the carbonyl and ring modes. The diagonal peaks obscure some of the cross-peaks, which might be improved with appropriate window functions.[8,23] The relative intensities of the cross-peaks change in ⟨0°,90°,90°,0°⟩ due to nonzero angles between their transition dipoles.[8,24] Peaks E and F are more clearly observed for ⟨45°,-45°,90°,0°⟩, which removes the diagonal peaks.[25] Cross-peaks also contribute to D that cause the residual "diagonal" peak in Figure 1d.

To interpret and simulate the spectra, we use an excitonic Hamiltonian that has previously been used to describe the

10.1021/jp035473h CCC: $25.00
Published on Web 08/12/2003

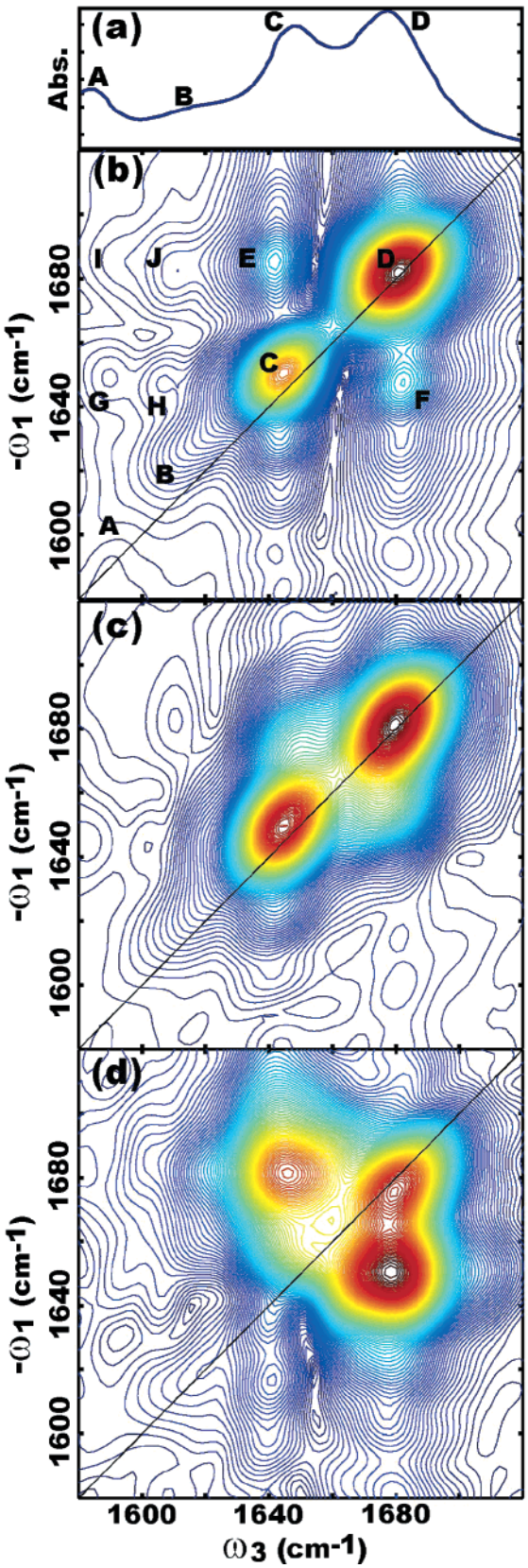

Figure 1. Normalized linear and heterodyned 2D-IR spectra of dG_5C_5: (a) linear spectrum (b) ⟨0°,0°,0°,0°⟩ (c) ⟨0°,90°,90°,0°⟩ and (d) ⟨45°,−45°,90°,0°⟩. The spectra are normalized to their peak heights and the contour lines are shown in 1% intervals. Peaks A−D are diagonal peaks and peaks E−J are cross-peaks. The diagonal peaks obscure most of the cross-peaks below the diagonal. The relative intensities of the cross-peaks in (b) and (c) depend on the angles between the transition dipoles. Only cross-peaks appear in (d), because the polarization condition eliminates the diagonal peaks.

amide-I band of peptides.[1] In the limit that the carbonyl group vibrations are completely separable from all other molecular modes, the vibrational Hamiltonian for the one-quantum exciton system of $dG_n{\cdot}dC_n$ can be written

$$^1H = \sum_i {}^{G}\epsilon_i|G_i\rangle\langle G_i| + \sum_i {}^{C}\epsilon_i|C_i\rangle\langle C_i| + \sum_{i<j} {}^{C}\beta_{ij}|C_i\rangle\langle C_j| + \sum_{i<j} {}^{G}\beta_{ij}|G_i\rangle\langle G_j| + \sum_{i,j} {}^{GC}\beta_{ij}(|C_i\rangle\langle G_j| + |G_j\rangle\langle C_i|) \quad (1)$$

where ${}^{G}\epsilon$ and ${}^{C}\epsilon$ are the site-energies for the G and C vibrational modes, ${}^{C}\beta$ and ${}^{G}\beta$ are the intrastrand couplings between stacked bases, and ${}^{GC}\beta$ are the interstrand couplings. The coupling terms β could be electrostatic or mechanical in nature. Diagonalization of ^1H gives the fundamental frequencies in the linear spectrum. Frequencies for the combination and overtone states of the cytidine bases can be attained from a similar expression for the two-quantum Hamiltonian that has the matrix elements

$$\langle 2C_i|^2H|2C_i\rangle = 2^{C}\epsilon_i - {}^{C}\Delta_i \qquad \langle C_iC_j|^2H|C_iC_j\rangle = {}^{C}\epsilon_i + {}^{C}\epsilon_j$$

$$\langle C_iC_j|^2H|C_iC_k\rangle = {}^{C}\beta_{jk} \qquad \langle C_iC_j|^2H|2C_j\rangle = \sqrt{2}{}^{C}\beta_{ij}$$

$$\langle C_iG_j|^2H|C_iG_j\rangle = {}^{C}\epsilon_i + {}^{G}\epsilon_j \qquad \langle C_iG_j|^2H|C_iC_k\rangle = {}^{GC}\beta_{jk}$$

$$\langle C_iG_j|^2H|2C_i\rangle = \sqrt{2}{}^{GC}\beta_{ij} \quad (2)$$

where $|2C_i\rangle$ is the two-quantum overtone state of $|C_i\rangle$ and ${}^{C}\Delta_i$ is the anharmonicity. The matrix elements for the guanosine sites and the remaining combination bands are obtained by replacing $|2C\rangle$ and $|CC\rangle$ with $|2G\rangle$ and $|GG\rangle$ in eq 2. The 2D-IR spectra are calculated from ^1H and ^2H.

Insight into the linear and 2D-IR spectra is obtained by considering two possible coupling limits. First, consider the interstrand coupling between the hydrogen-bonded bases, ${}^{GC}\beta_{ii}$, to be much larger than all other couplings. This may be the situation, because isotope labeling studies on poly(dG)·poly(dC) found ${}^{GC}\beta_{ii} = 15\ cm^{-1}$.[16] In this case, eq 1 is block diagonal and reduces to

$$^1H = n\begin{bmatrix} {}^{G}\epsilon & {}^{GC}\beta \\ {}^{GC}\beta & {}^{C}\epsilon \end{bmatrix} \quad (3)$$

As a result, the infrared spectra will be identical to that of two coupled oscillators. The two-quantum Hamiltonian also reduces to that of a coupled two-oscillator system,[4,8] and the 2D-IR spectrum contains diagonal and cross-peaks, as simulated in Figure 2a.

Second, consider the situation that the intrastrand couplings are much stronger than the interstrand couplings, i.e., ${}^{G}\beta$ and ${}^{C}\beta \gg {}^{GC}\beta$. This could be the situation if the coupling is electrostatic, because the intrastrand distances between the carbonyls of stacked bases are smaller than between carbonyls of hydrogen-bonded bases, especially for G, i.e., ${}^{GG}r = 3.3$, ${}^{CC}r = 4.7$, and ${}^{GC}r = 4.9$ Å for A-form DNA.[26] In this case, the last summation in eq 1 can be neglected and the Hamiltonian is again block diagonal. For an infinite helix, each block only has three infrared allowed transitions: one that is parallel to the helix axis, and two degenerate modes that are perpendicular to the axis.[27] For cytidine, their frequencies are given by ${}^{C}\epsilon_{\parallel}(\chi) = {}^{C}\epsilon_0 + \sum_n {}^{C}\beta_{i,i+n}$ and ${}^{C}\epsilon_{\perp}(\chi) = {}^{C}\epsilon_0 + \sum_n {}^{C}\beta_{i,i+n}\cos(n\chi)$ where $\chi = 2\pi/N$ and N is the number of oscillators per turn of the helix.[28] The relative strengths of these two bands are determined by the angle of the transition dipole moment to the helix axis.[29] A similar expression gives the guanosine frequen-

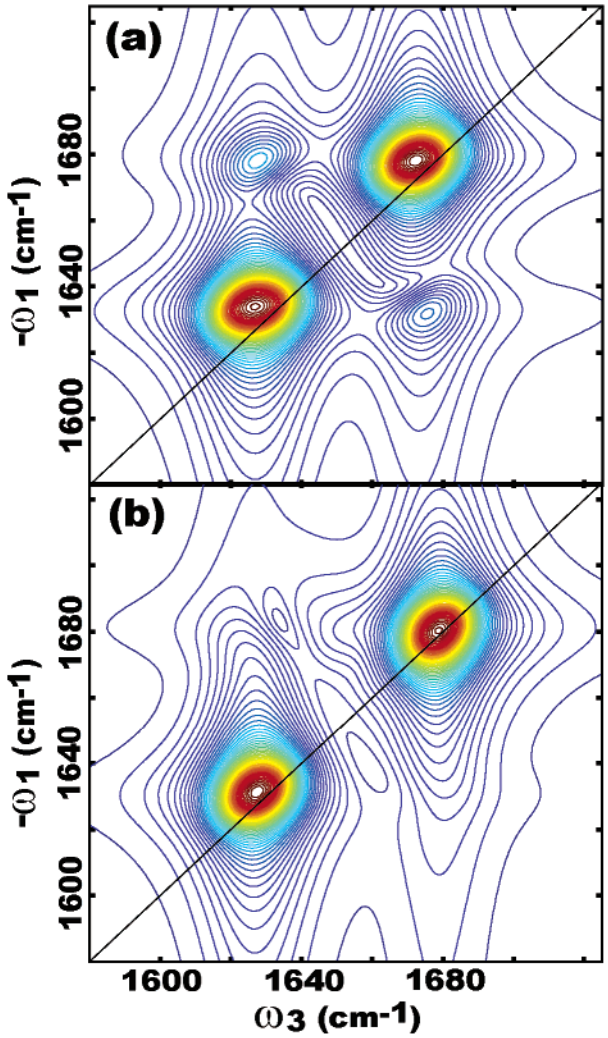

Figure 2. Simulated 2D-IR spectra in the limit that (a) the interstrand coupling is much larger than intrastrand, i.e., ${}^{GC}\beta \gg {}^{G}\beta$ and ${}^{C}\beta$, and (b) no interstrand coupling, i.e., ${}^{GC}\beta = 0$. Cross-peaks between the C and G vibrators are only observed when interstrand coupling is present.

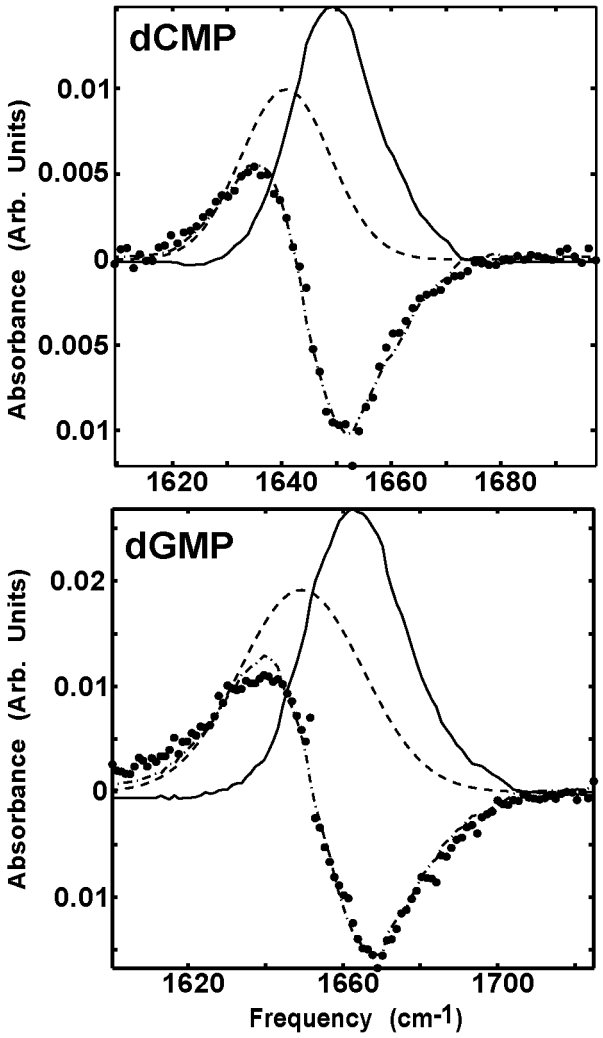

Figure 3. Fit of the pump−probe difference spectrum (dots) collected with a delay of T = 400 fs. The linear-infrared spectrum (solid) was used to model the bleach and stimulated emission, a Lorentzian was used for the new $v = 1 \rightarrow 2$ absorption (dashed), and the fit (dot−dashed) is also shown.

cies. It is expected that only the first term contributes significantly, because electrostatic coupling scales as $1/r^3$ and only adjacent bases can be mechanically coupled. Thus, when considering that A-form DNA has 10 basepairs per turn and that the bases are tilted 41° to the helix axis, the dominant transitions will have frequencies at ${}^{G}\epsilon_{\perp}(\chi) = {}^{G}\epsilon_0 + {}^{G}\beta_{i,i+1}$ and ${}^{C}\epsilon_{\perp}(\chi) = {}^{C}\epsilon_0 + {}^{C}\beta_{i,i+1}$. If ${}^{G}\beta_{i,i+1} > 0$, ${}^{C}\beta_{i,i+1} < 0$, and $|{}^{G}\beta_{i,i+1}| = |{}^{C}\beta_{i,i+1}|$, the fundamental frequencies would be indistinguishable from those for strong ${}^{GC}\beta_{ii}$, discussed above, limiting the usefulness of linear spectroscopy.

In general, ${}^{C}\beta_{i,i+1}$ and ${}^{G}\beta_{i,i+1}$ will not be equal or have the same sign, and the G and C transitions could lie at any frequency. For example, ${}^{C}\beta_{i,i+1} = 0$ and ${}^{G}\beta_{i,i+1} = 18$ cm^{-1} reproduce the fundamental frequencies of dG_5C_5. However, no matter how strong the intrastrand coupling, cross-peaks do not appear in the 2D-IR spectra when there is no interstrand coupling (Figure 2b). On the other hand, ${}^{GC}\beta$ alone is not sufficient to reproduce the spectra, because the cytidine frequency would shift upon helix formation. Thus, it appears that the coupling is between these two limits, and that both intra and interstrand couplings participate.

Interpreting the 2D-IR spectra with respect to the two coupling cases above indicates that both inter and intrastrand vibrational couplings are significant, but the origin of the coupling is still not clear. The coupling could be due to mechanical motions through the hydrogen bonds or electrostatic interactions between the transition dipoles. To test the latter case, the linear and 2D-IR spectra were self-consistently fit by diagonalizing ${}^{1}H$ and ${}^{2}H$ (eq 1 and 2) for $dG_5{\cdot}dC_5$ using a transition dipole coupling model, where $\beta_{ij} = (\vec{\mu}_i{\cdot}\vec{\mu}_j - 3(\vec{n}_{ij}{\cdot}\vec{\mu}_i)(\vec{n}_{ij}{\cdot}\vec{\mu}_j))/r_{ij}^3$; $\vec{\mu}_i$ are the transition dipoles, and $\vec{n}_{ij}$ are unit vectors connecting the two sites along the vector $\vec{r}_{ij}$. The site energies ${}^{G}\epsilon$ and ${}^{C}\epsilon$ are 1650 and 1664 cm^{-1}, respectively, taken from the linear spectra of dGMP and dCMP, which were also integrated to determine the transition dipole strengths $|{}^{G}\mu| = 3.9$ and $|{}^{C}\mu| = 3.6$ D·Å^{-1}·amu$^{-1/2}$. To ascertain the frequency shift caused by hydrogen bonding between basepairs, density functional calculations were performed on the base monomers with and without a methylamine group held at the position of the amino group in the opposing base.[30] Shifts of −0.8 to 1.8 cm^{-1} were found for the C and G bases, respectively, indicating that basepairing has little effect on the site energies, and were thus neglected. The transition dipoles were placed midway along the carbonyl bond using the canonical structure of A-form DNA.[26] The anharmonicities, ${}^{G}\Delta = 14$ and ${}^{C}\Delta = 9$ cm^{-1} were determined by fitting the pump−probe spectra of dCMP and dGMP (Figure 3). The only adjustable parameters in the model

are the angles of the transition dipoles relative to the carbonyl groups, ${}^{G}\theta$ and ${}^{C}\theta$, which were constrained to lie in the plane of the base, and the line shapes.[31]

The fits to the linear and 2D-IR spectra are shown in Figure 4 and are in good agreement with the experimental spectra. The fits give ${}^{G}\theta = -79°$ and ${}^{C}\theta = 14°$,[32] intrastrand couplings of ${}^{C}\beta_{i,i+1} = 2.3$ and ${}^{G}\beta_{i,i+1} = 9.7$ cm^{-1}, and interstrand coupling between hydrogen-bonded bases of ${}^{GC}\beta_{ii} = -7.4$ cm^{-1}. All other couplings are <1 cm^{-1} except for ${}^{GC}\beta_{i,i+1} = -5.0$ cm^{-1}.[33] As predicted by the simplified Hamiltonians above, there is significant interstrand coupling, but intrastrand coupling between stacked G bases is also very strong. Density functional calculations of the bases find that the normal modes include the C═O stretch, NH_2 scissor, and ring deformation,[34] suggesting that the transition dipoles do not lie directly on the carbonyl bond. The model could be refined by varying the position of the transition dipole, as has been done with the amide-I band of proteins.[13]

For an infinitely long helix, only three modes are infrared allowed, but in a finite helix the oscillator strength is spread over multiple modes. For five basepairs, diagonalization of ${}^{1}H$ with transition dipole coupling gives four strong transitions, two for G and two for C (Figure 4a, dashed). They are not resolved in the 2D-IR spectra because they are separated by less than the line widths, but they do cause the profile of the "diagonal" peaks to narrow in $\langle 0°,90°,90°,0°\rangle$ vs $\langle 0°,0°,0°,0°\rangle$ because they have cross-peaks between them that are apparent in $\langle 45°,-45°,90°,0°\rangle$. The cross-peaks between C and D contain transitions between all four modes.

The above simulations do not account for population or coherence transfer that might occur during the time scale of the experiment. Because the 2D-IR spectra are collected with $t_2 = 0$, the coherence generated during t_1 is immediately reversed for the time t_3, and as a result, population transfer can only occur for ~200 fs when the k_2 and k_3 laser pulses are overlapped. We estimate that less than 10% of the population can transfer during this time, because the lifetime of dCMP is measured to be ~1.3 ps with pump−probe spectroscopy. A small effect is also expected for coherence transfer.

Diagonal and off-diagonal disorder has also been neglected in the simulations. Because hydrogen bonding between bases does not appreciably alter the carbonyl frequencies, variations in the structure of the duplexed DNA probably has little effect on the diagonal disorder. However, structural variations should significantly alter the off-diagonal anharmonicities because the inter and intrastrand couplings are so strong. More insight into the off-diagonal disorder may come from 2D-IR spectra of the nonrephasing diagrams that, by comparison to the spectra given here, would give information on the correlation of the fluctuations between the G and C bands.[7,35,36] The simulations presented here assume purely correlated fluctuations.

An excitonic Hamiltonian for the carbonyl modes is only precisely correct when the carbonyl band forms an isolated subset of frequencies. Though this may be largely true, the ring vibrations of the bases are also coupled to the carbonyl stretches, as evidenced by peaks G−J in Figure 1. The off-diagonal anharmonicities of these peaks are roughly 0.2 cm^{-1}, on the basis of the linear scaling to the diagonal peaks. As a result, it may be possible to consider the ring couplings as a perturbation to the carbonyl bands. However, it is interesting to note that peak J is due to coupling of the cytosine ring stretch to the guanosine carbonyl mode, which is presumably an effect of mechanical coupling through the hydrogen-bonding network. The ring mode intensities also decrease upon duplex formation.

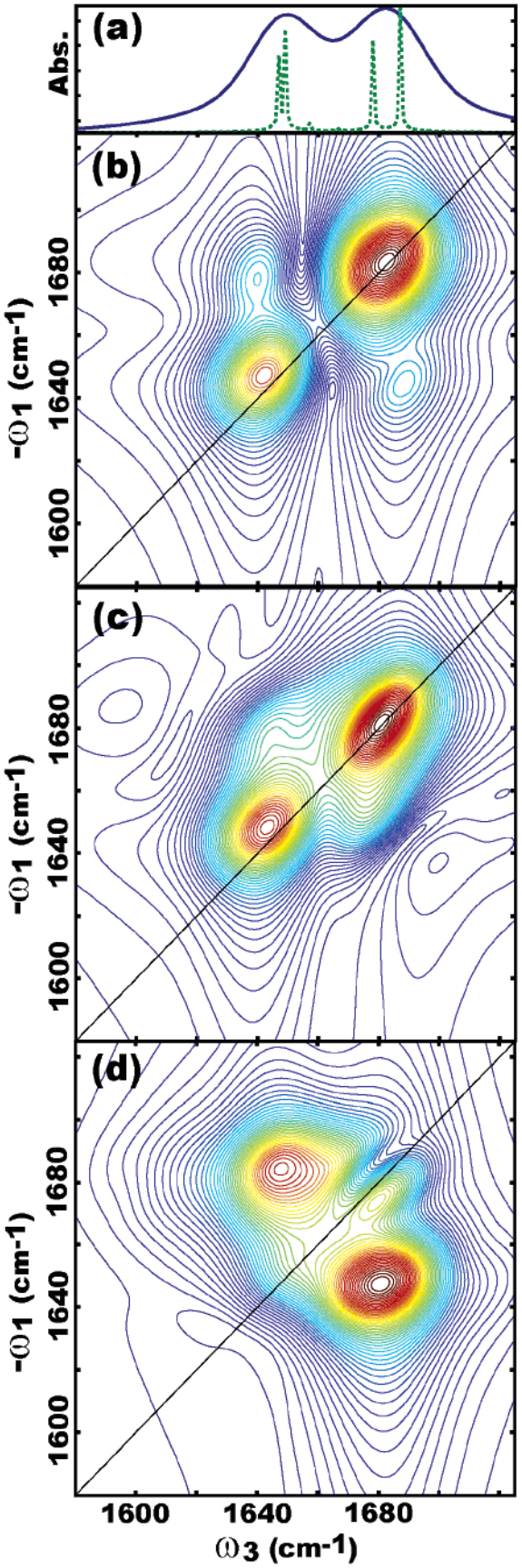

Figure 4. Fit to the linear and 2D-IR spectra using transition dipole coupling and the excitonic Hamiltonian of eq 1 and 2 for $dG_5{\cdot}dC_5$: (a) linear, (b) $\langle 0°,0°,0°,0°\rangle$ (c) $\langle 0°,90°,90°,0°\rangle$ and (d) $\langle 45°,-45°,90°,0°\rangle$. In (a), the best fit spectrum (solid) and the individual transitions (dashed) are shown. The spectra are normalized to their peak heights and the contour lines are shown in 2% intervals.

Better understanding of the ring modes will improve the coupling model.

In conclusion, the first 2D-IR spectrum of DNA was obtained. We observed cross-peaks between the G and C carbonyl bands that are interpreted as interstrand coupling across the two oligomers, and strong intrastrand coupling between stacked G carbonyls is also present. The spectra appear consistent with a transition dipole coupling model, but more experimental and theoretical work needs to be done to understand the role of mechanical coupling. Because adenosine−thymidine basepairs also contain carbonyl groups, it appears promising that a similar approach might provide a quantitative understanding of DNA infrared spectroscopy.

Acknowledgment. This research was supported by the Dreyfus Foundation, the Research Corporation, and the Wisconsin Alumni Research Foundation. A.T.K. thanks Troy Stich for helping with the UVCD. We also thank the reviewers for very helpful comments.

References and Notes

(1) Hamm, P.; Lim, M.; Hochstrasser, R. M. *J. Phys. Chem. B* **1998**, *102*, 6123.
(2) Iwaki, L. K.; Dlott, D. D. *J. Phys. Chem. A* **2000**, *104*, 9101.
(3) Zhao, W.; Wright, J. C. *Phys. Rev. Lett.* **2000**, *84*, 1411.
(4) Golonzka, O.; Khalil, M.; Demirdöven, N.; Tokmakoff, A. *Phys. Rev. Lett.* **2001**, *86*, 2154.
(5) Hybl, J. D.; Albrecht Ferro, A.; Jonas, D. M. *J. Chem. Phys.* **2001**, *115*, 6606.
(6) Stenger, J.; Madsen, D.; Hamm, P.; Nibbering, E. T. J.; Elsaesser, T. *Phys. Rev. Lett.* **2001**, *87*, 027401.
(7) Thompson, D. E.; Merchant, K. A.; Fayer, M. D. *J. Chem. Phys.* **2001**, *115*, 317.
(8) Zanni, M. T.; Gnanakaran, S.; Stenger, J.; Hochstrasser, R. M. *J. Phys. Chem. B* **2001**, *105*, 6520.
(9) Kaufman, L. J.; Heo, J.; Ziegler, L. D.; Fleming, G. R. *Phy. Rev. Lett.* **2002**, *88*, 207402/1.
(10) Piryatinski, A.; Tretiak, S.; Chernyak, V.; Mukamel, S. *J. Raman Spectrosc.* **2000**, *31*, 125.
(11) Cho, M. *J. Chem. Phys.* **2001**, *115*, 4424.
(12) Herzberg, G. *Infared and Raman spectra of polyatomic molecules*; D. Van Nostrand Co.: New York, 1945.
(13) Torii, H.; Tasumi, M. *J. Chem. Phys.* **1993**, *96*, 3379.
(14) Taillandier, E.; Liquier, J. *Methods Enzymol*, **1992**, *211*, 307.
(15) Liquier, J.; Taillandier, E. Infrared Spectroscopy of nucleic acids. In *Infrared Spectroscopy of Biomolecules*; Mantsch, H. H., Chapman, D., Eds.; Wiley-Liss: New York, 1996; p 131.
(16) Howard, F. B.; Frazier, J.; Miles, H. T. *Proc. Natl. Acad. Sci. U.S.A.* **1969**, *64*, 451.
(17) Tsuboi, M.; Takahashi, S. Infrared and Raman spectra of nucleic acids − vibrations in the base-residues. In *Physicochemical properties of nucleic acids*; Duchesne, J., Ed.; Academic Press: London, 1973; Vol. 2, p 91.
(18) Manuscript in preparation.
(19) The t_1 and t_3 delays were scanned 2000 and 3000 fs, respectively, in 18 fs steps. The signal-to-noise ratio is approximately 150:1.
(20) The samples were places between CaF_2 plates spaced 25 μm apart resulting in optical densities near 0.1.
(21) A-form was determined using UV circular dichroism, which has a positive peak at 260 nm, zero at 246 nm, and is independent of salt concentration between 50 mM and 1 M for 100 μM dG_5C_5. The crystal structure of dG_4C_4 is A-form (Eisenstein, M.; Shakked, Z. *J. Mol. Biol.* **1995**, *248*, 662).
(22) The ratio of the G diagonal peaks in $\langle 0°,0°,0°,0° \rangle$ and $\langle 0°,90°,-90°,0° \rangle$ is 2.5. The theoretical ratio is 3.0 for single oscillators, but cross-peaks are also present, as discussed with regard to $\langle 45°,-45°,90°,0° \rangle$.
(23) Zanni, M. T.; Asplund, M. C.; Hochstrasser, R. M. *J. Chem. Phys.* **2001**, *114*, 4579.
(24) Golonzka, O.; Tokmakoff, A. *J. Chem. Phys.* **2001**, *115*, 297.
(25) Zanni, M. T.; Ge, N.-H.; Kim, Y. S.; Hochstrasser, R. M. *Proc. Natl. Acad. Sci. U.S.A.* **2001**, *98*, 11265.
(26) Arnott, S.; Hukins, D. W. L. *Biochem. Biophys. Res. Commun.* **1972**, *47*, 1504.
(27) Higgs, P. W. *Proc. R. Soc. (London)* **1953**, *A220*, 472.
(28) Miyazawa, T. *J. Chem. Phys.* **1960**, *32*, 1647.
(29) Moffitt, W. *J. Chem. Phys.* **1956**, *25*, 467.
(30) Geometry optimization and frequency calculations were performed with Gaussian 98 using density functional theory with B3LYP functionals and 6-31+G(d) basis functions.
(31) 2D line shapes were generated by Fourier transforming the nonlinear response for a single oscillator in the Bloch limit. See ref 23. The best fit line shapes had homogeneous and inhomogeneous widths of 17 and 15 cm^{-1}, respectively.
(32) Clockwise and counterclockwise, respectively, in structure I.
(33) Systematic error makes it hard to determine the uncertainty of the parameters. However, changing either ${}^{G}\theta$ or ${}^{C}\theta$ by 10° gave a significantly poorer fit.
(34) Santamaria, R.; Charro, E.; Zacarías, A.; Castro, M. *J. Comput. Chem.* **1999**, *20*, 511.
(35) Ge, N.-H.; Zanni, M. T.; Hochstrasser, R. M. *J. Phys. Chem. A* **2002**, *106*, 962.
(36) Demirdoven, N.; Khalil, M.; Tokmakoff, A. *Phy. Rev. Lett.* **2002**, *89*, 237401/1.